BIOLOGY OF REPRODUCTION **81,** 921–932 (2009)
Published online before print 1 July 2009.
DOI 10.1095/biolreprod.109.076273

The Glycosylphosphatidylinositol-Anchored Serine Protease PRSS21 (Testisin) Imparts Murine Epididymal Sperm Cell Maturation and Fertilizing Ability[1]

Sarah Netzel-Arnett,[3] Thomas H. Bugge,[4] Rex A. Hess,[5] Kay Carnes,[5] Brett W. Stringer,[6] Anthony L. Scarman,[7] John D. Hooper,[7] Ian D. Tonks,[6] Graham F. Kay,[6] and Toni M. Antalis[2,3]

Center for Vascular and Inflammatory Diseases and the Department of Physiology,[3] University of Maryland School of Medicine, Baltimore, Maryland
Proteases and Tissue Remodeling Unit,[4] National Institute of Dental and Craniofacial Research, National Institutes of Health, Bethesda, Maryland
Reproductive Biology and Toxicology,[5] Department of Veterinary Biosciences, University of Illinois, Urbana, Illinois
Queensland Institute of Medical Research,[6] Herston, Queensland, Australia
Institute of Health and Biomedical Innovation,[7] Queensland University of Technology, Kelvin Grove, Queensland, Australia

ABSTRACT

An estimated 25%–40% of infertile men have idiopathic infertility associated with deficient sperm numbers and quality. Here, we identify the membrane-anchored serine protease PRSS21, also known as testisin, to be a novel proteolytic factor that directs epididymal sperm cell maturation and sperm-fertilizing ability. PRSS21-deficient spermatozoa show decreased motility, angulated and curled tails, fragile necks, and dramatically increased susceptibility to decapitation. These defects reflect aberrant maturation during passage through the epididymis, because histological and electron microscopic structural analyses showed an increased tendency for curled and detached tails as spermatozoa transit from the corpus to the cauda epididymis. Cauda epididymal spermatozoa deficient in PRSS21 fail to mount a swelling response when exposed to hypotonic conditions, suggesting an impaired ability to respond to osmotic challenges facing maturing spermatozoa in the female reproductive tract. These data suggest that aberrant regulation of PRSS21 may underlie certain secondary male infertility syndromes, such as "easily decapitated" spermatozoa in humans.

[1]Supported by the Lance Armstrong Foundation (T.M.A.); National Institutes of Health (NIH) grants CA098369 and HL084387 to T.M.A. and HL07698 to S.N.-A., the NIH Intramural program (T.H.B.); Department of Defense grant DAMD-17-02-1–0693 to T.H.B.; and the National Health and Medical Research Council (T.M.A. and G.F.K.). Partial support was provided by Consortium for Industrial Collaboration in Contraceptive Research (CICCR), a program of Contraceptive Research and Development (CONRAD), Eastern Virginia Medical School, to R.A.H. The views expressed by the authors do not necessarily reflect the views of CONRAD or CICCR. The National Institute of Child Health and Human Development (NICHD) Brain and Tissue Bank for Developmental Disorders at the University of Maryland School of Medicine and NICHD contracts N01-HD-4–3368 and N01-HD-4–3383 are acknowledged for deidentified human tissues.
[2]Correspondence: Toni M. Antalis, The Center for Vascular and Inflammatory Diseases, University of Maryland School of Medicine, 800 West Baltimore St., Baltimore, MD 21201. FAX: 410 706 8121; e-mail: tantalis@som.umaryland.edu

Received: 17 January 2009.
First decision: 18 February 2009.
Accepted: 16 June 2009.

eISSN: 1259-7268 http://www.biolreprod.org
ISSN: 0006-3363

decapitated sperm, easily decapitated sperm, epididymis, fertilizing ability, male reproductive tract, PRSS21, serine protease, sperm, sperm maturation, testisin

INTRODUCTION

The acquisition of sperm-fertilizing ability that occurs during epididymal maturation is critical for male fertility. Infertility affects up to 10% of human males, with the vast majority of cases due to insufficient sperm production and deficiencies in sperm quality [1]. Although spermatozoa are structurally developed in the testis, they are dependent on passage through the epididymis to acquire fertilization capability [2]. During epididymal transit, spermatozoa are functionally and morphologically matured to enable progressive motility and the ability to undergo capacitation, the series of biochemical and physiological changes that occur in sperm while in the female reproductive tract that are necessary for fertilization [3, 4]. These processes are dependent on a specialized luminal fluid microenvironment for maturing sperm along the entire epididymal duct and on changes in the spermatozoon, including the remodeling of the sperm plasma membrane.

Many molecular changes that occur during sperm maturation involve structural proteins, surface receptors, hormones, cytokines, water and ion channels, and extracellular matrix proteins, the activity and availability of which would be regulated by proteases [5–7]. As spermatozoa transit the epididymis, a number of sperm proteins are proteolytically processed to their mature forms [8], although to date, most of the specific proteases that are involved are unknown. A large number of tryptic serine proteases are present throughout the male reproductive tract [9]. These enzymes are distinguished by a catalytic triad of histidine (His), aspartate (Asp), and serine (Ser) residues in the active site, which are necessary for proteolytic activity [9]. The tryptic serine proteases also exhibit preference for cleavage of peptide substrates after basic (Arg/Lys) amino acids [5]. Substantial indirect evidence exists for the participation of tryptic serine proteolytic activities throughout spermatogenesis [10, 11] and during fertilization [12–18], suggesting multiple roles for these enzymes in the regulation of sperm development and function. The acrosomal serine protease, acrosin, was long considered to be critical for fertilization by mediating limited proteolysis of the oocyte zona pellucida (ZP), the extracellular matrix surrounding the oocyte, required for sperm penetration. However, acrosin

deficiency in mice did not prevent fertilization [18, 19], and penetration of acrosin-deficient sperm through the ZP could still be inhibited by a competitive inhibitor of trypsinlike serine proteases, *p*-aminobenzamidine (pAB) [14].

These data suggest that additional serine proteases play important roles in the regulation of male fertility. We and others previously identified PRSS21 (also referred to as testisin, esp-1, tryptase 4, and TESP5 [20–25]) as a tryptic serine protease abundantly expressed by male germ cells and sperm [20, 22], which is also present in capillary endothelial cells [26] and in eosinophils [21]. The gene (*PRSS21*) belongs to a distinct family of genes on the syntenic regions of human chromosome 16p13.3 and mouse chromosome 17 [22–24, 27] that includes genes encoding the serine proteases, prostasin, γ-tryptase, and pancreasin, each containing a hydrophobic peptide domain at their carboxy terminus [28]. PRSS21 is posttranscriptionally modified by the addition of a carboxy-terminal glycosylphosphatidylinositol membrane anchor [24]. Importantly, PRSS21 is pAB inhibitable and present within lipid rafts on the sperm plasma membrane [24], suggesting it may participate in sperm-egg interactions required for fertilization.

Here, we show that PRSS21 imparts epididymal sperm maturation and fertilizing ability to mammalian spermatozoa. Mutant mouse sperm lacking PRSS21 display several functional abnormalities, including an increased tendancy toward decapitation, heterogeneity in sperm form and angulated flagella, decreased numbers of motile sperm, and abnormal sperm volume regulation, all contributing to a decreased ability to fertilize oocytes. Defects occur during epididymal transit, suggesting an essential requirement for PRSS21 during sperm cell maturation processes required for fertilizing ability. Mice lacking PRSS21 further demonstrate reduced male fertility in short-term fertility studies. Collectively, these data provide developmental evidence specifically linking PRSS21 to the maturation and function of mammalian spermatozoa, opening new possibilities for our understanding of mammalian secondary fertility syndromes.

MATERIALS AND METHODS

Human Tissues

Deidentified human tissues were obtained from the National Institute of Child Health and Human Development Brain and Tissue Bank for Developmental Disorders at the University of Maryland School of Medicine under ethics protocols approved by the University of Maryland Institutional Review Board.

Immunoblot Analysis

Human and mouse tissues were disrupted in lysis buffer containing 1% Nonidet P-40. Cleared lysates were separated on a 4%–12% NuPAGE Bis-Tris Gel (Invitrogen), transferred to polyvinylidene fluoride, and immunoblotted using a monoclonal antibody raised to recombinant human PRSS21 (testisin; DD-P104 C37; diaDexus Inc., South San Francisco, CA) that detects both human and murine PRSS21 proteins. Protein concentrations were determined by the Bio-Rad assay. Antibody bound to the membrane was detected with horseradish peroxidase-conjugated goat anti-mouse antibody, with subsequent development using chemiluminescence (Supersignal; Pierce). As a control for loading, blots were stripped and reprobed with an anti-β-actin antibody (Santa Cruz Biotechnology).

Histopathology, Immunohistochemistry, and Electron Microscopy

For histopathological analysis of mice, organs were weighed and then fixed in 4% paraformaldehyde or Bouin fixative overnight prior to paraffin embedding. In some cases, animals were administered a lethal dose of anesthesia, and tissues were fixed by whole-body perfusion prior to tissue removal. The University of Maryland School of Medicine Institutional Animal Care and Use Committee approved all animal care and experimental procedures. Deparaffinized sections were stained with hematoxylin and eosin, or toluidine blue for light microscopic analysis to highlight cytology. Systematic morphological comparisons of the mouse testes were performed according to the criteria outlined by Oakberg [29] as modified in Russell et al. [30]. For immunohistochemistry, sections were deparaffinized and immersed in methanol containing 0.3% H_2O_2 for 30 min to exhaust endogenous peroxidase activity. After thorough washing, the sections were preincubated with 10% horse serum, followed by anti-PRSS21 (testisin) monoclonal antibody (DD-P104 C37) at 8 μg/ml for 1 h at room temperature. After washing in PBS, biotinylated anti-mouse immunoglobulin G was applied for 30 min at room temperature. The sections were washed thoroughly in PBS before incubation in Vectastain ABC reagent (Vector Laboratories, Burlingame, CA) for 30 min at room temperature. Sections were developed by incubation in 0.05% 3,3′-diaminobenzidine in Tris-HCl, pH 7.4, buffer with H_2O_2 as substrate. After washing in water, the sections were lightly counterstained with Mayer hematoxylin. Negative controls were stained as above but with PBS substituted for the primary antibody.

For transmission electron microscopy (TEM), tissue blocks were postfixed in 1% osmium tetroxide in 0.1 M cacodylate buffer containing 1.5% potassium ferrocyanide and were embedded in epoxy resin. Sections (1 μm) were stained with toluidine blue for light microscopy evaluation and photography prior to making ultrathin sections that were stained with uranyl acetate and lead citrate. The TEM photographs were made with a Hitachi H-800MU electron microscope.

Sperm Analyses

Male mice (10–12 wk old) were anesthetized, and the cauda of the epididymis was removed and placed in a 30-mm Petri dish containing WBB, which consists of 0.5 ml of prewarmed Whitten bicarbonate (WB) medium (109 mM NaCl, 4.7 mM KCl, 1.2 mM $MgSO_4$, 1.2 mM KH_2PO_4, 22 mM $NaHCO_3$, 5.5 mM glucose, 0.23 mM sodium pyruvate, 4.8 mM calcium lactate, 0.01 mg/ml gentamycin, and 0.001% phenol red; pH 7.4) plus 15 mg/ml bovine serum albumin (BSA). The osmolality of WBB is ~280 mmol/kg and is hypoosmotic relative to the cauda of murine epididymis (~410 mmol/kg) [31]. Sperm were released by a gentle nicking of the epididymides and incubated for 15 min at 37°C in 5% CO_2. Tissue was then removed, and sperm-containing supernatant was collected. Counts of total recovered spermatozoa were obtained by rendering an aliquot of spermatozoa immobile by submersion in a 65°C water bath for 2 min, and spermatozoa counted were determined using a hemocytometer after trypan blue staining.

For quantitative analysis of spermatozoa morphology, spermatozoa were released from nicked caput or caudal epididymides into HS media (135 mM NaCl, 5 mM KCl, 2 mM $CaCl_2$, 1 mM $MgCl_2$, 30 mM HEPES, 10 mM glucose, 10 mM lactic acid, and 1 mM pyruvic acid; pH 7.4) and incubated for 15 min at 37°C, and glutaraldehyde was added immediately to 5% final volume. Documentation of spermatozoa head and tail morphologies was performed by counting at least 200 recovered intact spermatozoa per animal by phase-contrast light microscopy. The spermatozoa were assessed as linear, angulated (bent greater than 90° or hairpin), or headless. Some morphological assessments were performed by drying spermatozoa-containing droplets (5 μl) on Superfrost slides (Fisher Scientific), fixing in cold methanol, and assessing structures using phase microscopy.

For quantitative assessment of sperm motility, cauda spermatozoa were released from nicked caudal epididymides into HS media plus 5 mg/ml BSA for 15 min at 37°C, and a sample was loaded onto a Cell-Vu Counting Chamber (Millennium Sciences Corp., New York, NY) prewarmed to 37°C. Sperm motilities, assessed by counting the number of intact sperm that were inactive, active but with no forward velocity, or active with forward velocity, were characterized as immotile, nonprogressive, and progressive, respectively, in a given field of view, with a total of 200 spermatozoa counted per animal. Headless sperm (flagellating tails alone) or separated sperm heads were not counted in these analyses. Motility characteristics were analyzed by computer-assisted sperm analyses of caudal spermatozoa released after a single nick for 3 min at 37°C into PBS (137 mM NaCl, 2.7 mM KCl, and 10 mM phosphate buffer; pH 7.4) plus 15 mg/ml BSA using an IVOS Spermatozoa Analyzer (Pathology Associates, Frederick, MD). The following kinematic parameters were measured: the vigor of movement, the average path velocity (VAP), the speed of forward progression, the amplitude of lateral head displacement, beat-cross frequency, and linearity of swim path.

In Vitro Fertilization

Oocytes were isolated from the oviducts and cumulus cells of superovulated (SOV) female, 2- to 4-mo-old 129/Sv mice at 16 h after human chorionic

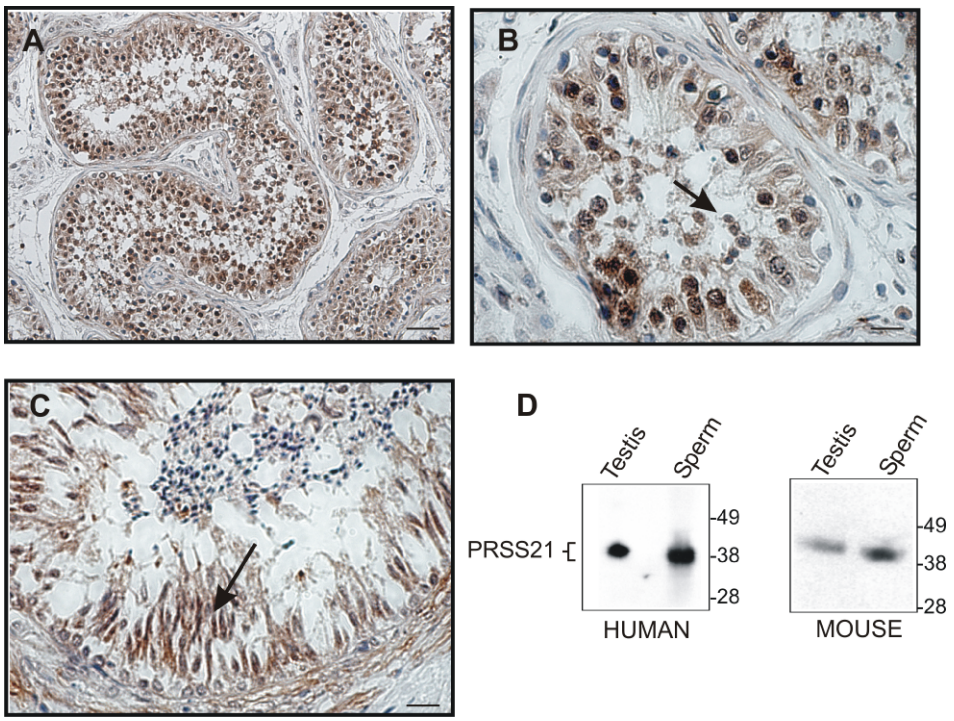

FIG. 1. PRSS21 is a human spermatozoa protein. **A**) PRSS21 immunostaining of spermatozoa (brown) in seminiferous tubules of human testis. **B** and **C**) PRSS21 immunostaining of cross-sections of human testis tissue showing positive staining of spermatids (**B**) and maturing sperm (**C**), as indicated by arrows. Bars = 50 μm (**A**) and 10 μm (**B** and **C**). **D**) Immunoblot analyses of PRSS21 in protein lysates prepared from human testis and human ejaculate spermatozoa, compared with lysates prepared from mouse testis and murine epididymal spermatozoa. Numbers indicate molecular weight standards in kDa.

gonadotropin (hCG), and they were removed into M2 medium, pH 7.4, supplemented with 2 mg/ml hyaluronidase. Isolated and washed caudal epididymides from adult *Prss21*$^{-/-}$ or wild-type littermates (approximately 5 mo old) were nicked and spermatozoa released into WB for 15 min at 37°C. Washed spermatozoa were capacitated in WBB for 90 min at 37°C in 5% CO_2. Equal numbers of wild-type and knockout (KO) spermatozoa (10 000 in 50 μl) were added to a 200-μl microdroplet containing 10–12 eggs in KSOM+AA medium, pH 7.4 (Specialty Media). Oocytes were exposed to spermatozoa for 3 h, after which point they were washed and transferred to fresh media, where they were cultured at 37°C and 5% CO_2 under equilibrated mineral oil. Eggs were examined after 24 h for the development of two-cell-stage embryos.

Spermatozoa Protein Phosphorylation

Caudal epididymal spermatozoa (1×10^6 of each genotype) were recovered in noncapacitating buffer (HS) or capacitating buffer (WBB) and incubated for the times indicated before the spermatozoa were recovered and the proteins extracted in lysis buffer and subjected to SDS-PAGE and immunoblotting using anti-phosphotyrosine antibody (Clone 4G10; Upstate Biotechnology Inc.) [32] or anti-phosphoserine/threonine antibody (Cell Signaling Technology) [33].

Measurement of Spermatozoa Volume by Light-Scatter Flow Cytometry

Spermatozoa cell volumes were measured by light-scatter flow cytometry as described previously [31]. Immediately (within 2 min) or 30 min after dispersion of spermatozoa in WBB at 37°C, an aliquot of the spermatozoa suspension (approximately 2×10^6 to 10×10^6 spermatozoa per milliliter) was diluted into the same media (without BSA) containing 3 μl of propidium iodide (PI) stock (0.5 mg/ml). Each spermatozoa sample was analyzed by flow cytometry under laser excitation at 488 nm (FACScan; Becton Dickinson). With cellular debris and aggregates gated out, forward- and side-scatter signals of the PI-negative cells were collected. Results are given in units of forward scatter (channel number) directly as measured and percentage of total spermatozoa.

Mating and Fertility

Male fertility was evaluated in postpubertal mice at approximately 10–20 wk. Continuous mating involved multiple inseminations during the course of several weeks. Short-term mating studies were performed using wild-type or *Prss21*$^{-/-}$ littermates (two groups of each genotype, with six mice in each group), each housed with two C57BL6/J female mice. The female mice were monitored twice daily for vaginal plug formation, at which time they were removed and monitored separately for pregnancies.

In Vivo Fertilization

Immature female 129/Sv mice were superovulated with 5 units of equine chorionic gonadotropin (Sigma) followed after 47 h by 5 units of hCG (Sigma). Immediately after the injection of hCG, female mice were mated with age-matched mice of each genotype. The next morning, female mice with vaginal plugs were removed from cages. Oocytes from females were removed from the uterus 3.5 days after hCG injection by using M2 medium, pH 7.4, supplemented with 2 mg/ml Type IV-S hyaluronidase (Sigma). Zygotes were examined for evidence of fertilization as determined by the presence of cell division and/or blastocyst formation.

Statistical Analyses

Student *t*-test was used to compare averages of normally distributed data with equal variance. Chi-square analysis was used for analysis of frequency distributions. The nonparametric Mann-Whitney rank sum test was used for the difference between medians in two groups. A threshold of $P < 0.05$ was considered significant. All tests were two tailed.

Supplemental Material

Supplemental Data include Supplemental Experimental Procedures and Supplemental Figures S1 and S2 (available online at www.biolreprod.org).

RESULTS

PRSS21 Is a Human Sperm Protein

We originally reported that PRSS21 was highly expressed in human testis and specifically present in the cytoplasm and on the plasma membrane of premeiotic human spermatocytes, but not detected after the first meiotic division [20], whereas mouse PRSS21 was strongly present in postmeiotic spermatogenic cells [22] and is found on maturing sperm [24]. Our data were obtained using antibodies generated against peptides encoded by human *PRSS21* and murine *Prss21* cDNA sequences. Having now available monoclonal antibodies generated against

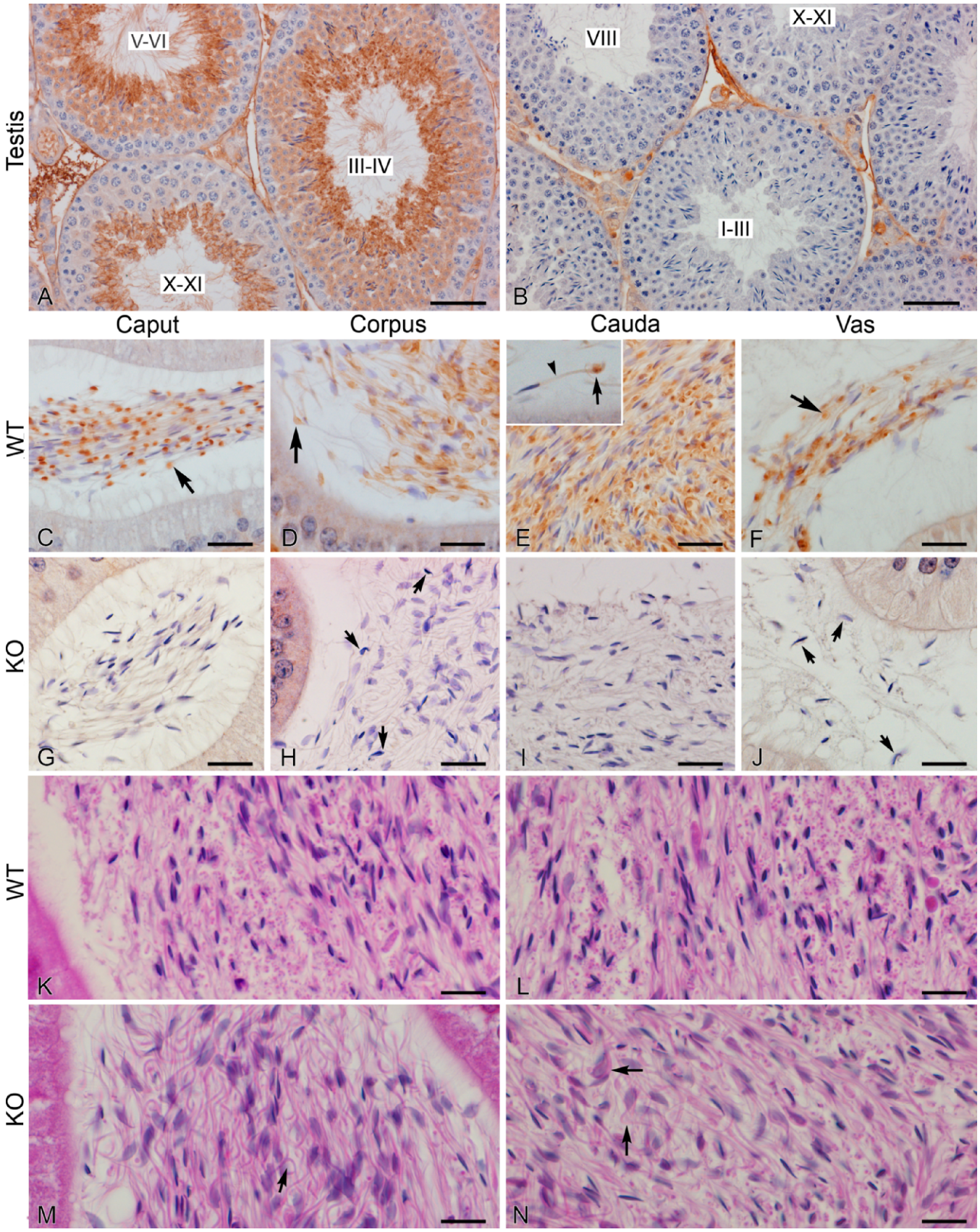

FIG. 2. Histopathology reveals abnormal cauda spermatozoa in *Prss21*$^{-/-}$ mice. **A**) Immunohistochemical staining of wild-type mouse testis. Strong positive staining is detected in the cytoplasm of round and elongated spermatids in several stages of spermatogenesis. Pachytene spermatocytes in stages X–XI also appear slightly positive. The tails of maturing spermatids that extend into the lumen also stain positive for PRSS21. **B**) Testis from a *Prss21*$^{-/-}$ mouse shows lack of PRSS21 expression throughout the seminiferous epithelium. **C**) Representative caput epididymis of a wild-type (WT) mouse showing PRSS21 staining of the cytoplasmic droplet of spermatozoa (arrow). **D**) Corpus epididymis of a wild-type mouse showing PRSS21 staining of the tail and

the full-length recombinant human PRSS21 protein [34], which detect both human and murine PRSS21 species, we reexamined PRSS21 expression in both humans and mice by immunostaining and Western blotting. Immunostaining of human testis tissue for PRSS21 using the anti-PRSS21 monoclonal antibody revealed specific PRSS21 staining on human spermatids throughout human spermatogenesis (Fig. 1, A–C), similar to its expression during murine spermatogenesis (Fig. 2A) [22]. Further confirmation of the presence of PRSS21 on mature human sperm was seen by immunoblot analysis, where the approximately 38- to 43-kDa PRSS21 protein was present both in human testes and in human ejaculate sperm (Fig. 1D). An as yet undefined posttranslational modification of human PRSS21 occurs in both human and mouse sperm compared with testis (resulting in a slightly faster migrating band), which has been reported previously in mice [24]. That PRSS21 remains present on human spermatogenic cells and mature sperm similarly to its expression in mice [22] and rats [35] suggests a similar function among these mammalian species.

Targeted Disruption of PRSS21 in Mice

To investigate PRSS21 function during male reproduction, we produced *Prss21*-null mice through disruption of the *Prss21* coding sequence by homologous recombination (detailed in Supplemental Experimental Procedures and Supplemental Fig. S1). Wild-type (+/+), heterozygous (+/−), and null (−/−) F(2) progeny were born at the expected Mendelian ratio of 1:2:1, respectively (n = 391; data not shown), indicating that PRSS21 is not essential for mouse development. All studies reported here were performed using age-matched littermates generated through heterozygous crosses. The *Prss21*$^{-/-}$ mice appear to develop normally and have developed no identifiable behavior abnormalities or obvious adverse phenotype. Weight gain of heterozygous and null mice occurred at a rate indistinguishable from that of wild-type littermates (data not shown). Examination of major organs and evaluation of blood cell counts and blood chemistries further revealed no significant differences due to PRSS21 deficiency (data not shown). Testes and epididymal weights of *Prss21*$^{-/-}$, heterozygous, and wild-type mice were similar (data not shown).

Abnormalities in Luminal Prss21$^{-/-}$ *Caudal Spermatozoa*

Detailed immunohistopathological analyses of *Prss21*$^{-/-}$ and wild-type testes revealed that even though PRSS21 is expressed within the seminiferous epithelium during all stages of spermatogenesis (Fig. 2A), no obvious abnormalities associated with testicular male germ cell development were identified in the *Prss21*$^{-/-}$ mice. Spermatogenesis appeared normal, and all stages of spermatogenesis were present (Fig. 2B and data not shown). In the epididymis of wild-type mice, PRSS21 staining was associated with the luminal spermatozoa from the caput through the corpus to the cauda regions of the epididymal tracts (Fig. 2, C–E), as well as spermatozoa present in the vas deferens (Fig. 2F). Specifically, PRSS21 antibodies stained the cytoplasmic droplet of epididymal spermatozoa, as well as the midpiece and neck (Fig. 2E, inset), as has been reported previously [24]. Although spermatozoa present in *Prss21*$^{-/-}$ caput epididymis were mostly normal (Fig. 2G), abnormalities appeared with the entry of *Prss21*$^{-/-}$ spermatozoa into the cauda epididymis, beginning in the lumen of the corpus epididymis (Fig. 2H) and continuing through passage to the cauda epididymis and vas deferens (Fig. 2, I and J). The *Prss21*$^{-/-}$ cauda epididymides contained a number of morphologically abnormal spermatozoa mixed with normal spermatozoa, and they did not show the tightly organized and directional alignment of cauda spermatozoa bundles typical of highly concentrated spermatozoa of their wild-type littermates (Fig. 2, K and L vs. M and N). These mutant spermatozoa were characterized by abnormally curled tails and random orientation of the heads and tails (Fig. 2, M and N, arrows).

The TEM analysis of *Prss21*$^{-/-}$ epididymides revealed numerous abnormalities in luminal *Prss21*$^{-/-}$ caudal spermatozoa. These consisted of curled tails, abnormally shaped heads, round bodies, and fused tails (Fig. 3, D and E compared with A–C). In addition, a significant number of spermatozoa heads present in the lumen of the *Prss21*$^{-/-}$ caudal epididymides appeared detached from tails. In contrast, spermatozoa present in caput epididymides of *Prss21*$^{-/-}$ mice appeared relatively normal (data not shown). Collectively, these data indicate defective maturation of luminal spermatozoa during passage through the epididymis [31, 36–39].

Prss21$^{-/-}$ *Mice Have Reduced Numbers of Viable Spermatozoa Due to Increased Decapitation*

To investigate the impact of the observed abnormalities in epididymal sperm maturation on sperm attributes, functional analyses were performed on cauda spermatozoa from *Prss21*$^{-/-}$ and wild-type epididymides released under standard conditions into hypotonic culture media. We noted that the counts of intact, viable cauda spermatozoa released from *Prss21*$^{-/-}$ cauda epididymides were consistently ~30% lower than the counts recovered from the wild-type counterparts (Fig. 4A), requiring additional numbers of *Prss21*$^{-/-}$ mice to obtain equivalent sperm numbers. The reduction in numbers of *Prss21*$^{-/-}$ released spermatozoa could not be accounted for by germ cell loss during spermatogenesis or loss of spermatozoa numbers during epididymal transit (Supplemental Fig. S2). Microscopic inspection of the cauda spermatozoa released from *Prss21*$^{-/-}$ and wild-type epididymides revealed that a high percentage of spermatozoan heads only (without tails) were present on the

cytoplasmic droplet (arrow). **E**) Cauda epididymis of wild-type mouse showing PRSS21 staining of highly concentrated spermatozoa. The inset photograph (original magnification ×60) shows a single spermatozoan with an attached cytoplasmic droplet (arrow), which is immunopositive. The arrowhead indicates the slight staining of the neck region of the spermatozoa. **F**) Vas deferens of a wild-type mouse showing PRSS21 staining of spermatozoa that remains intense along the cytoplasmic droplet (arrow) and neck regions. **G**) Caput epididymis of the *Prss21*$^{-/-}$ mouse showing lack of immunostaining. The spermatozoa are organized similarly to those in the wild-type lumen shown in **C**. **H**) Corpus epididymis of *Prss21*$^{-/-}$ mouse showing potentially abnormal spermatozoa heads (arrows). The spermatozoa appear to be more disorganized within the epididymal lumen, beginning in the corpus. **I**) Cauda epididymis of *Prss21*$^{-/-}$ mouse showing disorganization of the spermatozoa compared with wild-type cauda epididymis shown in **E**. **J**) Vas deferens of *Prss21*$^{-/-}$ mouse showing detached spermatozoa heads (arrows) and no staining for PRSS21. **K** and **L**) Representative photomicrographs of wild-type cauda epididymides stained with hemotoxylin and eosin. **M** and **N**) Representative photomicrographs of *Prss21*$^{-/-}$ cauda epididymides stained with hemotoxylin and eosin showing the ubiquitous presence of abnormally curled spermatozoa tails (as indicated by arrows). Bars = 50 μm (**A** and **B**) and 20 μm (**C**–**N**).

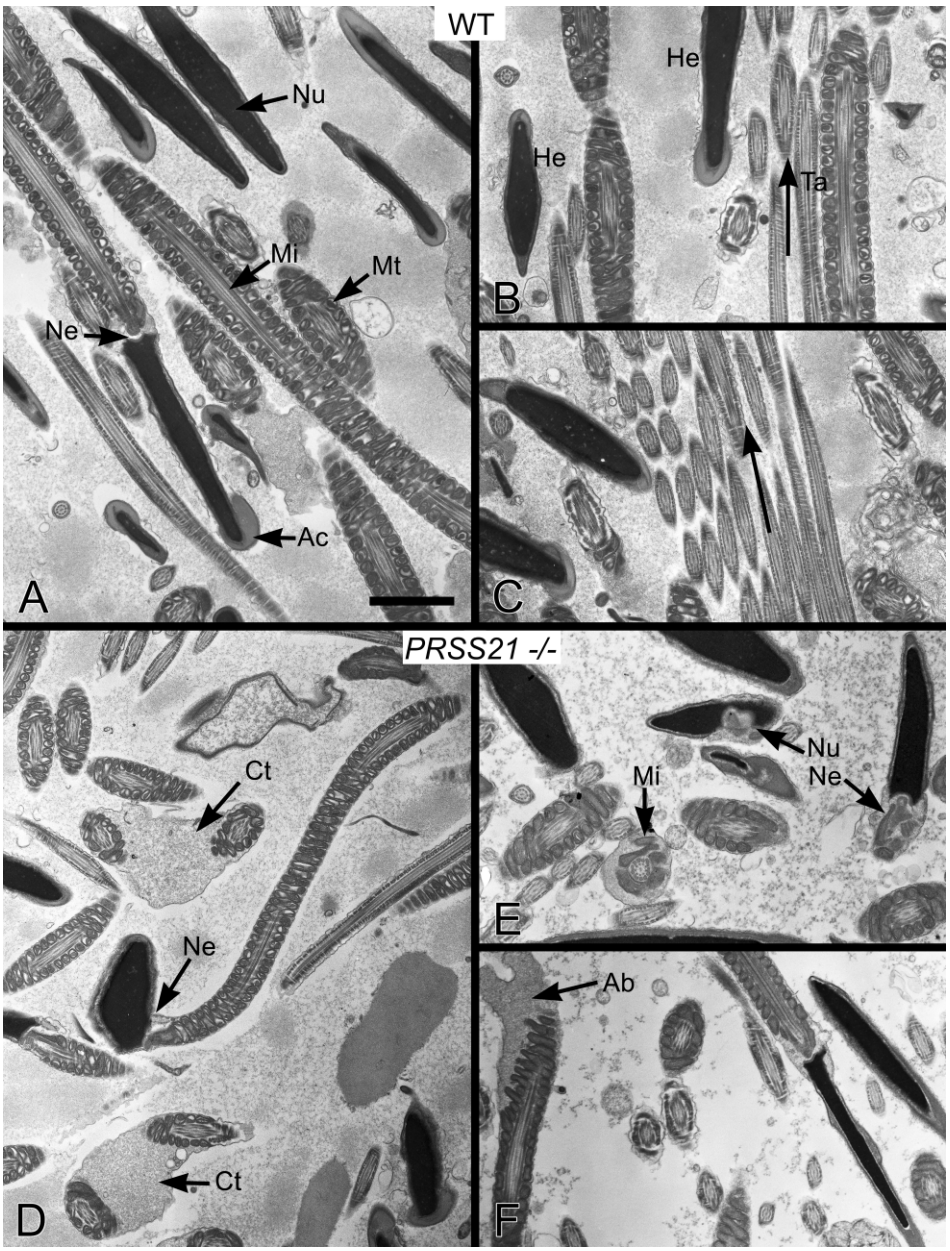

FIG. 3. Ultrastructural analysis by TEM of caudal luminal spermatozoa from wild-type (WT) and *Prss21*$^{-/-}$ mice. **A**) Wild type showing normal cauda spermatozoa sections through the nucleus (Nu), midpiece showing mitochondria (Mt) and microtubules (Mi), the neck connecting piece (Ne), and the acrosome (Ac). **B**) Wild-type spermatozoa showing alignment (arrow) of the spermatozoa heads (He) and tails (Ta). **C**) Wild-type spermatozoa showing a bundle of normal spermatozoa tails in alignment (arrow). **D**) *Prss21*$^{-/-}$ spermatozoa showing abnormal spermatozoa, including a head that is bent at the neck (Ne) and two coiled tail cross-sections (Ct). **E**) *Prss21*$^{-/-}$ spermatozoa showing abnormal spermatozoa head with indentation of the acrosome and nucleus (Nu), abnormal neck connecting piece (Ne), and abnormal mitochondrial placement in the midpiece (Mi). **F**) *Prss21*$^{-/-}$ spermatozoa showing another abnormal spermatozoa midpiece (Ab). Bar = 2 μm.

bottom of the culture dish, indicative of enhanced decapitation in the *Prss21*$^{-/-}$ spermatozoan population (Fig. 4B). Glutaraldehyde fixation of released *Prss21*$^{-/-}$ and wild-type spermatozoa showed the *Prss21*$^{-/-}$ population to be heterogeneous and highly variable, associated with a distinct ragged appearance, angulated tails, and hairpin conformations (Fig. 4C). Quantitation of caudal spermatozoa morphologies (Fig. 4D, left) revealed that less than 20% of the *Prss21*$^{-/-}$ spermatozoa possessed a normal linear conformation typical of caudal spermatozoa, with a vast majority showing an aberrant bend (angular) shape (~52%) or separation of heads from tails (~30%). The reduced counts of viable *Prss21*$^{-/-}$ caudal spermatozoa may be explained by these morphological abnormalities and the increased tendency for decapitation.

In contrast to cauda spermatozoa, spermatozoa released from *Prss21*$^{-/-}$ caput epididymides appeared morphologically similar to their wild-type couterparts (Fig. 4D, right), consistent with their normal appearance by histological analysis (Fig. 2G) and supporting the notion that maturation defects in *Prss21*$^{-/-}$ luminal spermatozoa occur during passage through the epididymis.

Prss21$^{-/-}$ *Cauda Spermatozoa Display Reduced Motility and Decreased Fertilization Capabilities*

Quantitative motility assessment of recovered intact cauda spermatozoa revealed significantly fewer numbers of spermatozoa exhibiting flagellar movement in the *Prss21*$^{-/-}$ population (~40%; Fig. 5A, left) compared with wild-type littermate controls. Of the motile spermatozoa subpopulation, only ~50% of the *Prss21*$^{-/-}$ spermatozoa demonstrated progressive motility in a forward direction (Fig. 5A, right). Kinematic analysis of the population of *Prss21*$^{-/-}$ spermatozoa exhibiting progressive motility did not reveal any significant abnormalities in motility characteristics (e.g., straight line velocity, curvilinear velocity, and VAP) compared with wild-type littermate controls (data not shown).

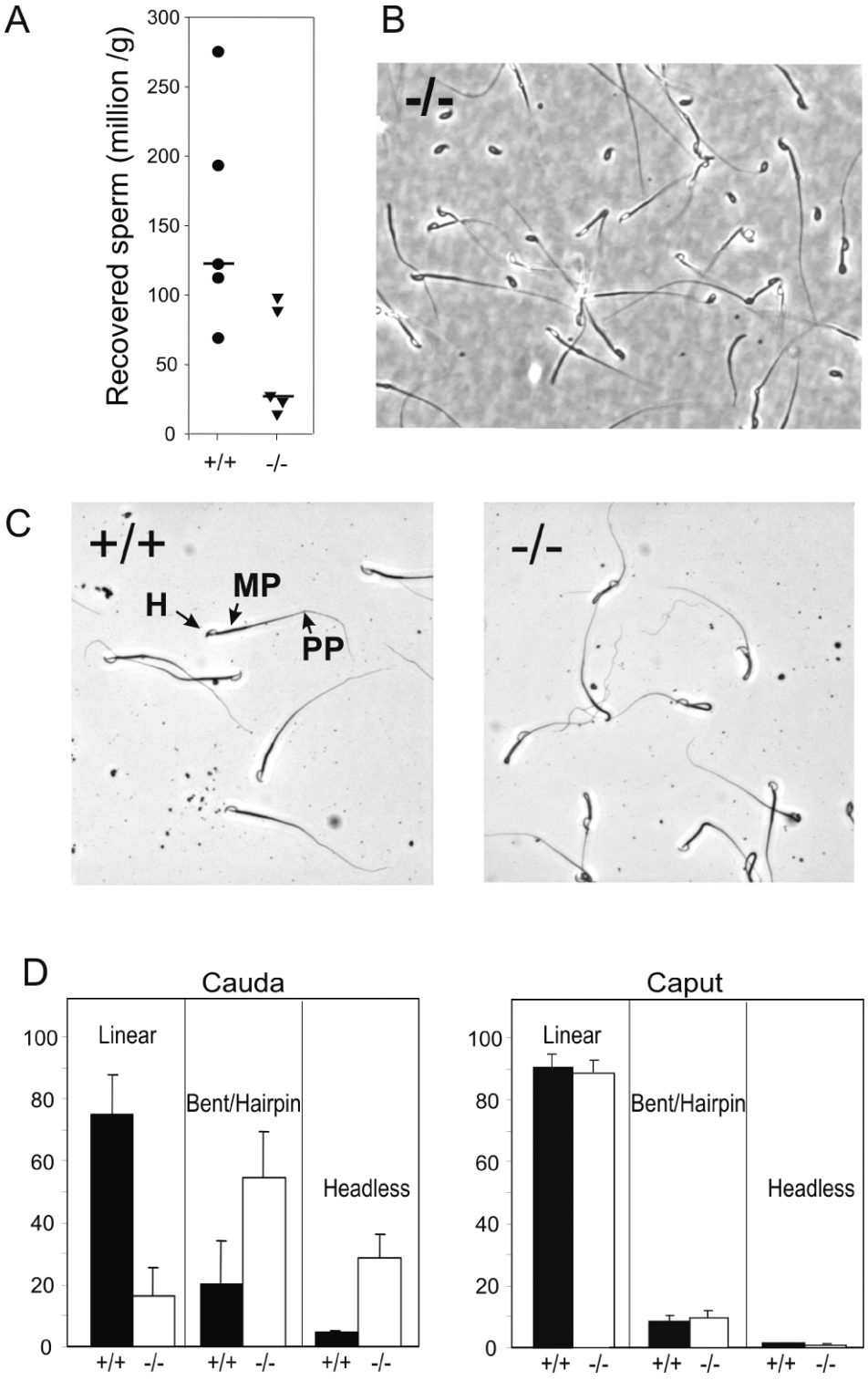

FIG. 4. *Prss21*$^{-/-}$ mice have reduced numbers of viable spermatozoa. **A**) Reduced recovery of spermatozoa released from *Prss21*$^{-/-}$ cauda epididymis. Spermatozoa were released from a single nick in isolated cauda for 15 min at 37°C prior to counting. Mean values are indicated by bars. ($^{+/+}$ vs. $^{-/-}$, $P \leq 0.05$ Mann-Whitney, two-tailed test). **B**) Photograph of the bottom of a culture dish taken under phase contrast showing increased separation of spermatozoa heads from tails in *Prss21*$^{-/-}$ spermatozoa released into WB media. **C**) Aberrant morphologies in *Prss21*$^{-/-}$ spermatozoa. Spermatozoa were released, air dried on slides, and fixed in methanol. More than 50% of the spermatozoa in this specimen from a *Prss21*$^{-/-}$ mouse exhibited the hairpin morphology, with the bend occurring at the cytoplasmic droplet between the midpiece and the principal piece. Head (H), midpiece (MP), and principal piece (PP) are as indicated. **D**) Quantitation of spermatozoa morphological abnormalities in glutaraldehyde-fixed spermatozoa released from cauda and caput epididymes as indicated. At least 200 spermatozoa per mouse of each genotype (n = 3) were counted by light microscopy. Y-axes represent percentage of total spermatozoa. Original magnification ×20 (**B**) and ×20 (**C**).

The fertilization competence of *Prss21*$^{-/-}$ spermatozoa compared with their wild-type counterparts was addressed by in vitro fertilization experiments. Wild-type and *Prss21*$^{-/-}$ caudal spermatozoa were released into capacitating media, and equal numbers of intact spermatozoa of each genotype were exposed to mature, ZP-intact oocytes for 3 h, after which the eggs were washed and transferred to fresh media. Oocyte fertilization, measured by the formation of two-cell embryos after 24 h, occurred at a reduced frequency with *Prss21*$^{-/-}$ spermatozoa compared with wild-type littermate controls (39% vs. 61%; Fig. 5B). These data indicate a reduced ability to initiate fertilization.

Sperm functions required for fertilization competence, the initiation of sperm motility, capacitation, and the acrosome reaction are critically regulated though the phosphorylation of specific proteins [4, 40–44]. Protein serine/threonine phosphorylation in mammalian sperm is considered to play an important role in the initiation and maintenance of sperm motility [33, 45–47]. In addition, tyrosine phosphorylation is strongly associated with the onset of sperm motility and

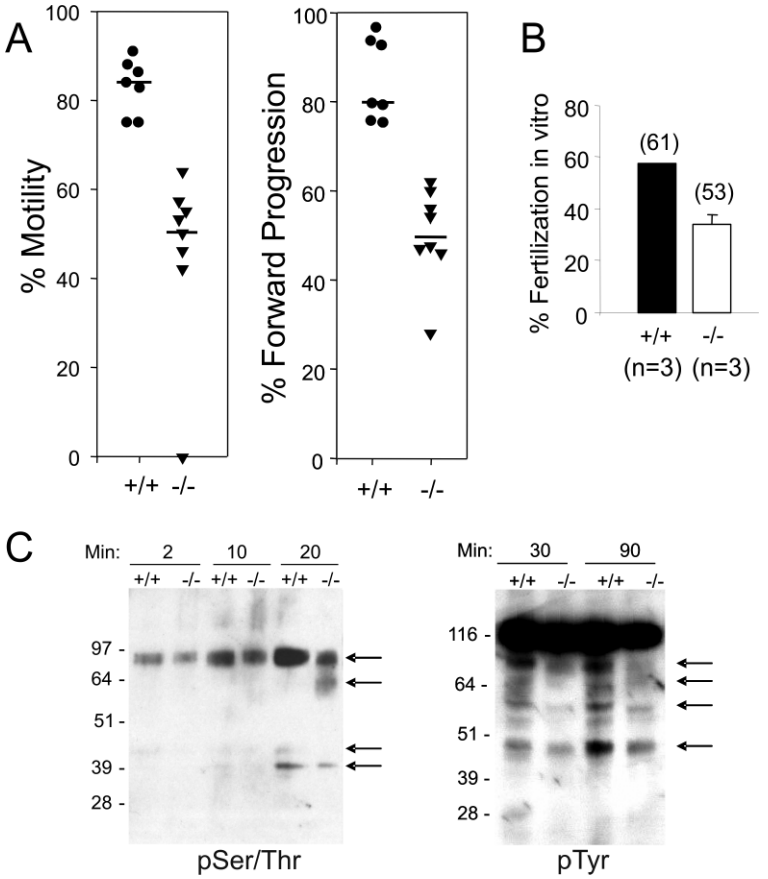

FIG. 5. PRSS21 cauda spermatozoa display reduced motility and decreased fertilization competence. **A**) Motility of *Prss21*$^{-/-}$ vs. wild-type control caudal spermatozoa (left). Spermatozoa released from isolated caudal epididymis into WBB and exhibiting flagellar motion (motile) were counted using Cell Vue counting chambers and are expressed as a percent of total spermatozoa. Median values are indicated by bars. ($^{+/+}$ vs. $^{-/-}$, $P \leq 0.02$ Mann-Whitney, two-tailed test). Percent forward progression of caudal spermatozoa (right). Released cauda spermatozoa with forward progressive movement are expressed relative to the total number of motile spermatozoa. Median values are indicated by bars. ($^{+/+}$ vs. $^{-/-}$, $P \leq 0.02$ Mann-Whitney, two-tailed test). **B**) *Prss21*$^{-/-}$ spermatozoa show reduced fertilization competence compared with wild-type littermate controls ($P \leq 0.05$, Mann-Whitney, two-tailed test). Eggs were prepared from SOV female 129/Sv mice and inseminated with capacitated spermatozoa from *Prss21*$^{-/-}$ or wild-type adult littermates for 3 h, followed by washing. The percent fertilization was determined by counting two-cell embryos at 24 h after insemination. The total number of oocytes analyzed is given in parentheses above each bar. **C**) Protein serine/threonine phoshorylation (pSer/Thr) and capacitation-associated tyrosine phosphorylation (pTyr) are decreased in *Prss21*$^{-/-}$ spermatozoa. Cauda spermatozoa from *Prss21*$^{-/-}$ or wild-type adult littermates were dispersed into noncapacitating (left) or capacitating (right) media for the times indicated. Sperm proteins were analyzed by immunoblotting using anti-phosphoserine or anti-phosphotyrosine antibodies as indicated. Numbers indicate molecular weight standards in kDa. The intense tyrosine-phosphorylated band is hexokinase [32]. Arrows indicate major proteins showing reduced phosphorylation.

capacitation [45, 46, 48, 49]. Wild-type cauda spermatozoa released into noncapacitating or capacitating media display a typical induction of protein serine/threonine and tyrosine phosphorylation (Fig. 5C) [50–52]. *Prss21*$^{-/-}$ cauda spermatozoa show substantially reduced serine/threonine phosphorylation and capacitation-associated tyrosine phosphorylation (Fig. 5C), consistent with a blunted fertilization capability in the *Prss21*$^{-/-}$ population.

Luminal Prss21$^{-/-}$ *Spermatozoa Display an Inability to Regulate Sperm Cell Volume Changes*

A functional attribute acquired during maturation of luminal spermatozoa as they transit the epididymis is the ability to regulate sperm cell volume [53–55]. Matured caudal spermatozoa released into hypotonic culture medium exhibit cell swelling, mechanisms of regulatory volume decrease (RVD), and other changes required for fertilization competence [56]. Immature caput spermatozoa do not exhibit cell swelling when exposed to hypotonic media. To address the functionality of *Prss21*$^{-/-}$ luminal spermatozoa, sperm cell volumes of cauda spermatozoa released into hypotonic media were measured by flow cytometric light-scatter analysis [31, 54, 57]. Upon exposure to hypotonic media, wild-type spermatozoa exhibited an immediate swelling response (within 2 min), reflected in an observed increase in forward light scatter (Fig. 6A). Sperm swelling was followed by an adaptive RVD response within 30 min (Fig. 6B) due to ion channel activation, a net loss of ions and water, and recovery of normal cell volume [55]. In contrast, *Prss21*$^{-/-}$ spermatozoa failed to mount an effective swelling response upon release into hypotonic media (Fig. 6C), and there was no change after 30 min (Fig. 6D). These data demonstrate that PRSS21 contributes to the ability of maturing sperm to respond to osmotic challenges, an attribute important for fertilization competence.

Prss21$^{-/-}$ *Male Mice Have a Fertility Defect*

When bred by continuous mating, the *Prss21*$^{-/-}$ mice displayed apparently normal fertility, and average litter sizes were similar between *Prss21*$^{-/-}$ and wild-type male mice (data not shown). To evaluate the specific reproductive performance

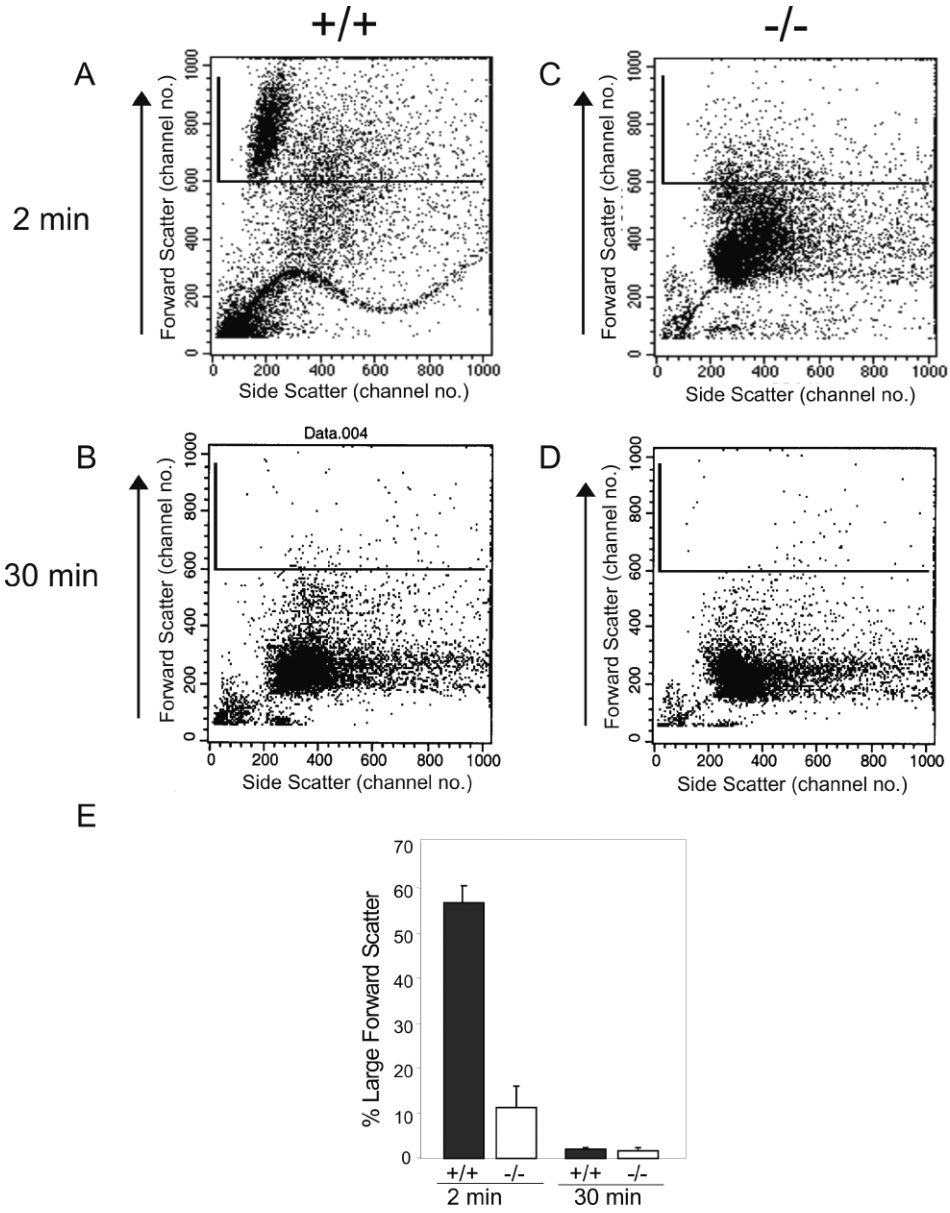

FIG. 6. *Prss21*$^{-/-}$ spermatozoa fail to respond to osmotic challenge. Representative dual-parameter dot plots from flow cytometric analyses showing the distribution of viable cauda spermatozoa according to their laser forward-scatter and side-scatter (90°C) signals. Cauda spermatozoa from wild-type *Prss21*$^{+/+}$ (**A** and **B**) or *Prss21*$^{-/-}$ (**C** and **D**) mice were released into hypotonic media, and measurements were taken immediately (within 2 min; **A** and **C**) or after 30 min (**B** and **D**). In each plot, representing one sperm sample, the window demarcates the subpopulation of sperm characterized by their large forward-scatter signals, an indicator of increasing cell volume (arrow). **E**) Percentage of viable spermatozoa with large forward scatter (increased volume) obtained from *Prss21*$^{-/-}$ (n = 4) and wild-type littermate control (n = 3) populations. *Prss21*$^{-/-}$ cauda spermatozoa fail to swell immediately upon release into hypotonic media, compared with wild-type control spermatozoa ($P < 0.002$, Student *t*-test). Values are means ± SEM.

of *Prss21*$^{-/-}$ spermatozoa, short-term mating studies were performed. Males of each genotype were paired with virgin C57BL6/J females (one male per two females), and the number of litters produced per plugged female was monitored. No differences in mating behavior or vaginal plug formation were observed between *Prss21*$^{-/-}$ and wild-type littermates. However, the *Prss21*$^{-/-}$ males demonstrated a significantly reduced number of pregnancies per plugged female (6/24) relative to their wild-type littermates (18/23; $P \leq 0.001$, chi-square test; Fig. 7A). To investigate whether this reduced reproductive performance was accompanied by decreased fertilization capabilities, *Prss21*$^{+/+}$ and *Prss21*$^{-/-}$ male littermates were paired with SOV females, and the development of blastocysts was monitored after 3.5 days as an index of fertilization. Although 92.2% (47/51) of eggs developed to blastocysts after SOV females were mated to *Prss21*$^{+/+}$ males, only 47.6% (39/82) of eggs from *Prss21*$^{-/-}$ littermates developed to the blastocyst/compacted morula stage (Fig. 7B). These data show that PRSS21 contributes to sperm function and fertilization capabilities in vivo.

DISCUSSION

The studies presented here reveal a role for the sperm membrane serine protease PRSS21 as a transducer of maturation cues imposed on spermatozoa during epididymal transit that are important for fertilizing ability. In both human and mice, PRSS21 is highly expressed on the surface of round and elongated spermatids of the testis, and it remains associated with the spermatozoa tail throughout the epididymal tract. PRSS21 deficiency in mice had no apparent effect on germ cell development in the testis, but instead led to defective maturation of epididymal sperm, resulting in a lower viable sperm count and and reduced sperm-fertilizing ability. PRSS21 deficiency produced a continuum of epididymal spermatozoa phenotypes ranging from dysfunctional (headless) to apparently normal motile spermatozoa. Morphologically, the spermatozoa population contained multiple abnormalities, with a ragged appearance and a substantial proportion of hairpinlike structures. Fertilizing ability was reduced, as reflected in reduced blastocyst formation both in vivo and in vitro, reduced capacitation capability, and impaired ability to respond to hyperosmotic challenge.

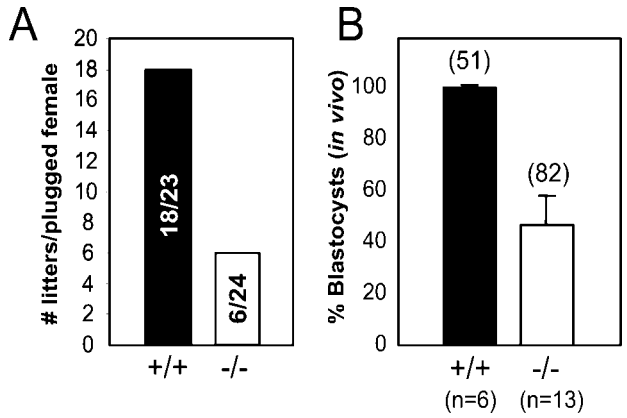

FIG. 7. PRSS21-deficient males show reduced male fertility. **A**) *Prss21*$^{-/-}$ mice are subfertile. Wild-type and knockout male littermates (10–20 wk old) were each paired with two C57BL6 females. After plug formation, females were removed and monitored for pregnancies. Pregnancies resulted in females from 78% of wild-type males (n = 23) vs. 25% of knockout males (n = 24); $P \leq 0.001$, chi-square. **B**) *Prss21*$^{-/-}$ spermatozoa show reduced fertilization capability in vivo. Wild-type (n = 6) and *Prss21*$^{-/-}$ (n = 13) male littermates were mated with immature SOV 129/Sv females, and the development of blastocysts was monitored after 3.5 days as described in *Materials and Methods*. The efficiency of blastocyst formation was monitored as an index of fertilization. *Prss21*$^{-/-}$ vs. $^{+/+}$, $P \leq 0.05$, Mann-Whitney, two-tailed test.

As mammalian spermatozoa traverse the epididymis to their site of temporary storage in the cauda, they encounter a progressive increase in osmotic fluids along its length to reach a level that is hyperosmotic relative to serum (~410 mmol/kg in the mouse), which is maintained in the cauda epididymis [55, 58]. The difference in osmotic pressure between the epididymal and uterine lumina necessitates an adjustment in cell volume as spermatozoa enter the relatively hypotonic female tract, which initiates diverse signaling mechanisms required for fertilization competence [55]. The absence of a rapid swelling response of released *Prss21*$^{-/-}$ cauda spermatozoa upon exposure to hypotonic media reflects a compromised ability to regulate sperm cell volume in the face of osmotic challenge.

This study expands our understanding of how sperm cell maturation is regulated and highlights an unexpected role for a sperm serine protease in this process. Prior studies on the prevention of fertilization by serine protease inhibitors have mostly focused on the acrosome reaction and the possible role of sperm serine proteases on the proteolytic lysis of the ZP during sperm penetration [24, 59]. A recent study by Yamashita et al. [60] identified a role for PRSS21 in sperm-egg binding and in the ability of sperm to fuse with an egg in vitro. PRSS21-deficient sperm had reduced sperm-egg binding and reduced ability to fertilize eggs in vitro, which could be partially rescued by exposure of *Prss21*$^{-/-}$ sperm to uterine fluids. Here, we identify a critical role for PRSS21 during epididymal sperm cell maturation that has an impact on sperm motility and fertilizing ability. Reduced motility of *Prss21*$^{-/-}$ sperm coincides with a reduction in both serine/threonine and tyrosine phosphorylation, events that are associated with the initiation of motility and capacitation of sperm. Our results may suggest another strategy by which PRSS21 may modulate sperm-fertilizing ability. Effective mechanical thrust is critical for sperm penetration of the oocyte ZP during fertilization in both mice and humans [59]. Thus, the combined impact of reduced sperm motility and reduced functional capabilities, secondary to defective epididymal maturation, would account for the reduced fertilization ability of PRSS21-deficient spermatozoa.

PRSS21 deficiency induces significant heterogeneity in the mature sperm population, although a sufficient percentage of *Prss21*$^{-/-}$ sperm appear morphologically normal and capable of fertilizing eggs. Remarkably, PRSS21 deficiency is deleterious to the structural integrity of mature sperm, suggesting that PRSS21 participates in a developmental pathway required for the integrity of the sperm head and tail. Similar heterogeneity has been reported as a result of haploinsufficiency of the gene encoding the protein kinase A type 1α regulatory subunit in mice on a mixed 129Sv/J genetic background. The cauda sperm of these mice are fragile, approximately half of them are decapitated, and intact sperm exhibit reduced motility [61]. "Easily decapitated" spermatozoa, abnormal morphologies, and hairpin structures are well-recognized secondary infertility syndromes in both humans and livestock [62–67]. The sperm phenotypes associated with PRSS21 deficiency in mice suggest that deficiencies in this enzyme either directly or indirectly could account for some cases of male secondary infertility. Whether PRSS21 on the sperm plasma membrane 1) contributes to the maintenance of the hyperosmotic state of luminal epididymal spermatozoa in the epididymis, 2) functions to maintain integrity of the sperm plasma membrane, and/or 3) contributes to mechanisms that control sperm cell volume regulation and/or phosphorylation are important areas for further investigation.

The abnormalities associated with PRSS21 deficiency are unique for a gene encoding a membrane-anchored serine protease, and they are more severe than has been observed in knockouts of other serine protease genes expressed in the male reproductive tract. Inactivation of the genes encoding proacrosin [19], plasminogen [68, 69], urokinase-type plasminogen activator, and tissue-type plasminogen activator [70] show no direct deleterious effect on fertility in mice. Genetic deficiency of proprotein convertase 4 (PCSK4), a serine protease expressed in round spermatids, leads to impaired fertility; however, no spermatogenic abnormalities were identified [71].

The proteolytic capability of PRSS21, its surface membrane localization, and its pattern of expression, may suggest that PRSS21 regulates proteolytic cleavage of a substrate(s) that regulates epididymal sperm maturation. The identity of this substrate is not known. Hepatocyte growth factor, also known as scatter factor, is expressed in the male genital tract and is activated by proteolytic enzymes related to PRSS21; its activation could mediate phosphorylation events through its receptor, MET (c-met), present on epididymal spermatozoa [72]. In addition, epithelial sodium channels (ENaCs), which regulate cell volume changes and fluid balance in other cells [73], are present in mouse spermatogenic cells and in mature sperm. Several other membrane serine proteases related to PRSS21, including prostasin, matriptase, and murine TMPRSS4, are implicated in proteolytic activation of ENaCs by a mechanism involving regulated release of inhibitory peptides from ENaC subunits [74]. Recent studies show that SCNN1A (ENaC-α) and SCNN1D (ENaC-δ) subunits contribute to hyperpolarization of the sperm plasma membrane during capacitation [75], which is required to render sperm competent for fertilization. Further studies are required to identify PRSS21 target substrates during epididymal sperm maturation and initiation of sperm motility.

Male infertility affects an estimated 6% of human males [76, 77]. Although some cases of male infertility occur as a consequence of anatomical abnormalities, the vast majority of cases are due to low sperm counts and reduced motility of unidentifiable causes [77]. PRSS21 is expressed by human

male germ cells throughout human spermatogenesis and is highly expressed by human sperm. A better understanding of the molecular mechanisms that regulate PRSS21 and sperm-fertilizing ability is important not only for treatment of male infertility syndromes, but it may also provide an approach to the development of male contraceptive methods based on interfering with epididymal sperm maturation. PRSS21 deficiency has provided new insight into a novel mechanism that is important for sperm maturation and likely to be of significance to causes of unexplained infertility syndromes in humans.

ACKNOWLEDGMENTS

We thank Professor Christian Haudenschild and Elizabeth Smith for assistance with histopathology; Trichia Murdock, Beth Burke, Marissa Kuhnen, and Brooke Curie for help with mouse husbandry; and the National Institute of Dental and Craniofacial Research Gene Targeting Core for blastocyst injections.

REFERENCES

1. Zhao C, Huo R, Wang FQ, Lin M, Zhou ZM, Sha JH. Identification of several proteins involved in regulation of sperm motility by proteomic analysis. Fertil Steril 2007; 87:436–438.
2. Trainer TD. Testis and excretory duct system. In: Sternberg SS (ed.), Histology for Pathologists. New York, NY: Raven Press; 1992:731–750.
3. Yanagimachi R. Fertility of mammalian spermatozoa: its development and relativity. Zygote 1994; 2:371–372.
4. Visconti PE, Westbrook VA, Chertihin O, Demarco I, Sleight S, Diekman AB. Novel signaling pathways involved in sperm acquisition of fertilizing capacity. J Reprod Immunol 2002; 53:133–150.
5. Rawlings ND, Barrett AJ. Families of serine peptidases. Methods Enzymol 1994; 244:19–61.
6. Puente XS, Sanchez LM, Overall CM, Lopez-Otin C. Human and mouse proteases: a comparative genomic approach. Nat Rev Genet 2003; 4:544–558.
7. Netzel-Arnett S, Hooper JD, Szabo R, Madison EL, Quigley JP, Bugge TH, Antalis TM. Membrane anchored serine proteases: a rapidly expanding group of cell surface proteolytic enzymes with potential roles in cancer. Cancer Metastasis Rev 2003; 22:237–258.
8. Cornwall GA, Lareyre JJ, Matusik RJ, Hinton BT, Orgebin-Crist MC. Gene expression and epididymal function. In: Robaire B, Hinton BT (eds.), The Epididymis: From Molecules to Clinical Practice. New York: Kluwer Academic/Plenum Publishers; 2002:169–199.
9. Barrett AJ, Rawlings ND, Woessner JF eds. Handbook of Proteolytic Enzymes, 2nd ed. London: Elsevier Academic Press; 2004.
10. Jones R, Ma A, Hou ST, Shalgi R, Hall L. Testicular biosynthesis and epididymal endoproteolytic processing of rat sperm surface antigen 2B1. J Cell Sci 1996; 109:2561–2570.
11. Phelps BM, Koppel DE, Primakoff P, Myles DG. Evidence that proteolysis of the surface is an initial step in the mechanism of formation of sperm cell surface domains. J Cell Biol 1990; 111:1839–1847.
12. Kohno N, Yamagata K, Yamada S, Kashiwabara S, Sakai Y, Baba T. Two novel testicular serine proteases, TESP1 and TESP2, are present in the mouse sperm acrosome. Biochem Biophys Res Commun 1998; 245:658–665.
13. Honda A, Siruntawineti J, Baba T. Role of acrosomal matrix proteases in sperm-zona pellucida interactions. Hum Reprod Update 2002; 8:405–412.
14. Yamagata K, Murayama K, Kohno N, Kashiwabara S, Baba T. p-Aminobenzamidine-sensitive acrosomal protease(s) other than acrosin serve the sperm penetration of the egg zona pellucida in mouse. Zygote 1998; 6:311–319.
15. Zaneveld LJ, Robertson RT, Kessler M, Williams WL. Inhibition of fertilization in vivo by pancreatic and seminal plasma trypsin inhibitors. J Reprod Fertil 1971; 25:387–392.
16. Miyamoto H, Chang MC. Effects of protease inhibitors on the fertilizing capacity of hamster spermatozoa. Biol Reprod 1973; 9:533–537.
17. Bhattacharyya AK, Goodpasture JC, Zaneveld LJ. Acrosin of mouse spermatozoa. Am J Physiol 1979; 237:E40–E44.
18. Yamagata K, Murayama K, Okabe M, Toshimori K, Nakanishi T, Kashiwabara S, Baba T. Acrosin accelerates the dispersal of sperm acrosomal proteins during acrosome reaction. J Biol Chem 1998; 273: 10470–10474.
19. Baba T, Azuma S, Kashiwabara S, Toyoda Y. Sperm from mice carrying a targeted mutation of the acrosin gene can penetrate the oocyte zona pellucida and effect fertilization. J Biol Chem 1994; 269:31845–31849.
20. Hooper JD, Nicol DL, Dickinson JL, Eyre HJ, Scarman AL, Normyle JF, Stuttgen MA, Douglas ML, Loveland KA, Sutherland GR, Antalis TM. Testisin, a new human serine proteinase expressed by premeiotic testicular germ cells and lost in testicular germ cell tumors. Cancer Res 1999; 59: 3199–3205.
21. Inoue M, Kanbe N, Kurosawa M, Kido H. Cloning and tissue distribution of a novel serine protease esp-1 from human eosinophils. Biochem Biophys Res Commun 1998; 252:307–312.
22. Scarman AL, Hooper JD, Boucaut KJ, Sit ML, Webb GC, Normyle JF, Antalis TM. Organization and chromosomal localization of the murine Testisin gene encoding a serine protease temporally expressed during spermatogenesis. Eur J Biochem 2001; 268:1250–1258.
23. Wong GW, Yasuda S, Madhusudhan MS, Li L, Yang Y, Krilis SA, Sali A, Stevens RL. Human tryptase epsilon (PRSS22), a new member of the chromosome 16p13.3 family of human serine proteases expressed in airway epithelial cells. J Biol Chem 2001; 276:49169–49182.
24. Honda A, Yamagata K, Sugiura S, Watanabe K, Baba T. A mouse serine protease TESP5 is selectively included into lipid rafts of sperm membrane presumably as a glycosylphosphatidylinositol-anchored protein. J Biol Chem 2002; 277:16976–16984.
25. Antalis TM, Boucaut KJ, Netzel-Arnett S. Testisin. In: Barrett AJ, Rawlings ND, Woessner JF Jr (eds.), Handbook of Proteolytic Enzymes, 2nd ed. London, UK: Elsevier; 2003:1702–1703.
26. Aimes RT, Zijlstra A, Hooper JD, Ogbourne SM, Sit ML, Fuchs S, Gotley DC, Quigley JP, Antalis TM. Endothelial cell serine proteases expressed during vascular morphogenesis and angiogenesis. Thromb Haemost 2003; 89:561–572.
27. Hooper JD, Bowen N, Marshall H, Cullen LM, Sood R, Daniels R, Stuttgen MA, Normyle JF, Higgs DR, Kastner DL, Ogbourne SM, Pera MF, et al. Localization, expression and genomic structure of the gene encoding the human serine protease testisin. Biochim Biophys Acta 2000; 1492:63–71.
28. Caughey GH, Raymond WW, Blount JL, Hau LW, Pallaoro M, Wolters PJ, Verghese GM. Characterization of human gamma-tryptases, novel members of the chromosome 16p mast cell tryptase and prostasin gene families. J Immunol 2000; 164:6566–6575.
29. Oakberg EF. A description of spermiogenesis in the mouse and its use in analysis of the cycle of the seminiferous epithelium and germ cell renewal. Am J Anat 1956; 99:391–414.
30. Russell LD, Ettlin RA, Sinha Hikim AP, Clegg ED. Histological and Histopathological Evaluation of the Testis. Clearwater, FL: Cache River Press; 1990.
31. Yeung CH, Anapolski M, Cooper TG. Measurement of volume changes in mouse spermatozoa using an electronic sizing analyzer and a flow cytometer: validation and application to an infertile mouse model. J Androl 2002; 23:522–528.
32. Visconti PE, Bailey JL, Moore GD, Pan D, Olds-Clarke P, Kopf GS. Capacitation of mouse spermatozoa. I. Correlation between the capacitation state and protein tyrosine phosphorylation. Development 1995; 121: 1129–1137.
33. O'Flaherty C, de Lamirande E, Gagnon C. Phosphorylation of the Arginine-X-X-(Serine/Threonine) motif in human sperm proteins during capacitation: modulation and protein kinase A dependency. Mol Hum Reprod 2004; 10:355–363.
34. Tang T, Kmet M, Corral L, Vartanian S, Tobler A, Papkoff J. Testisin, a glycosyl-phosphatidylinositol-linked serine protease, promotes malignant transformation in vitro and in vivo. Cancer Res 2005; 65:868–878.
35. Nakamura Y, Inoue M, Okumura Y, Shiota M, Nishikawa M, Arase S, Kido H. Cloning, expression analysis, and tissue distribution of esp-1/testisin, a membrane-type serine protease from the rat. J Med Invest 2003; 50:78–86.
36. Cho HW, Nie R, Carnes K, Zhou Q, Sharief NA, Hess RA. The antiestrogen ICI 182,780 induces early effects on the adult male mouse reproductive tract and long-term decreased fertility without testicular atrophy. Reprod Biol Endocrinol 2003; 1:57.
37. Cooper TG, Yeung CH, Wagenfeld A, Nieschlag E, Poutanen M, Huhtaniemi I, Sipila P. Mouse models of infertility due to swollen spermatozoa. Mol Cell Endocrinol 2004; 216:55–63.
38. Drevius LO, Eriksson H. Osmotic swelling of mammalian spermatozoa. Exp Cell Res 1966; 42:136–156.
39. Suzuki-Toyota F, Ito C, Toyama Y, Maekawa M, Yao R, Noda T, Toshimori K. The coiled tail of the round-headed spermatozoa appears during epididymal passage in GOPC-deficient mice. Arch Histol Cytol 2004; 67:361–371.

40. de Lamirande E, O'Flaherty C. Sperm activation: role of reactive oxygen species and kinases. Biochim Biophys Acta 2008; 1784:106–115.
41. Urner F, Sakkas D. Protein phosphorylation in mammalian spermatozoa. Reproduction 2003; 125:17–26.
42. Salicioni AM, Platt MD, Wertheimer EV, Arcelay E, Allaire A, Sosnik J, Visconti PE. Signalling pathways involved in sperm capacitation. Soc Reprod Fertil Suppl 2007; 65:245–259.
43. Tulsiani DR, Zeng HT, Abou-Haila A. Biology of sperm capacitation: evidence for multiple signalling pathways. Soc Reprod Fertil Suppl 2007; 63:257–272.
44. Naz RK, Rajesh PB. Role of tyrosine phosphorylation in sperm capacitation / acrosome reaction. Reprod Biol Endocrinol 2004; 2:75.
45. Tash JS, Bracho GE. Identification of phosphoproteins coupled to initiation of motility in live epididymal mouse sperm. Biochem Biophys Res Commun 1998; 251:557–563.
46. Turner RM. Moving to the beat: a review of mammalian sperm motility regulation. Reprod Fertil Dev 2006; 18:25–38.
47. Wade MA, Jones RC, Murdoch RN, Aitken RJ. Motility activation and second messenger signalling in spermatozoa from rat cauda epididymidis. Reproduction 2003; 125:175–183.
48. Ficarro S, Chertihin O, Westbrook VA, White F, Jayes F, Kalab P, Marto JA, Shabanowitz J, Herr JC, Hunt DF, Visconti PE. Phosphoproteome analysis of capacitated human sperm. Evidence of tyrosine phosphorylation of a kinase-anchoring protein 3 and valosin-containing protein/p97 during capacitation. J Biol Chem 2003; 278:11579–11589.
49. Visconti PE, Moore GD, Bailey JL, Leclerc P, Connors SA, Pan D, Olds-Clarke P, Kopf GS. Capacitation of mouse spermatozoa. II. Protein tyrosine phosphorylation and capacitation are regulated by a cAMP-dependent pathway. Development 1995; 121:1139–1150.
50. Si Y, Okuno M. Role of tyrosine phosphorylation of flagellar proteins in hamster sperm hyperactivation. Biol Reprod 1999; 61:240–246.
51. Osheroff JE, Visconti PE, Valenzuela JP, Travis AJ, Alvarez J, Kopf GS. Regulation of human sperm capacitation by a cholesterol efflux-stimulated signal transduction pathway leading to protein kinase A-mediated up-regulation of protein tyrosine phosphorylation. Mol Hum Reprod 1999; 5: 1017–1026.
52. Demarco IA, Espinosa F, Edwards J, Sosnik J, De La Vega-Beltran JL, Hockensmith JW, Kopf GS, Darszon A, Visconti PE. Involvement of a Na+/HCO-3 cotransporter in mouse sperm capacitation. J Biol Chem 2003; 278:7001–7009.
53. Yeung CH, Sonnenberg-Riethmacher E, Cooper TG. Infertile spermatozoa of c-ros tyrosine kinase receptor knockout mice show flagellar angulation and maturational defects in cell volume regulatory mechanisms. Biol Reprod 1999; 61:1062–1069.
54. Yeung CH, Anapolski M, Depenbusch M, Zitzmann M, Cooper TG. Human sperm volume regulation. Response to physiological changes in osmolality, channel blockers and potential sperm osmolytes. Hum Reprod 2003; 18:1029–1036.
55. Yeung CH, Barfield JP, Cooper TG. Physiological volume regulation by spermatozoa. Mol Cell Endocrinol 2006; 250:98–105.
56. Petrunkina AM, Harrison RA, Ekhlasi-Hundrieser M, Topfer-Petersen E. Role of volume-stimulated osmolyte and anion channels in volume regulation by mammalian sperm. Mol Hum Reprod 2004; 10:815–823.
57. Yeung CH, Anapolski M, Sipila P, Wagenfeld A, Poutanen M, Huhtaniemi I, Nieschlag E, Cooper TG. Sperm volume regulation: maturational changes in fertile and infertile transgenic mice and association with kinematics and tail angulation. Biol Reprod 2002; 67:269–275.
58. Turner TT. Spermatozoa are exposed to a complex microenvironment as they traverse the epididymis. Ann N Y Acad Sci 1991; 637:364–383.
59. Bedford JM. Mammalian fertilization misread? Sperm penetration of the eutherian zona pellucida is unlikely to be a lytic event. Biol Reprod 1998; 59:1275–1287.
60. Yamashita M, Honda A, Ogura A, Kashiwabara S, Fukami K, Baba T. Reduced fertility of mouse epididymal sperm lacking Prss21/Tesp5 is rescued by sperm exposure to uterine microenvironment. Genes Cells 2008; 13:1001–1013.
61. Burton KA, McDermott DA, Wilkes D, Poulsen MN, Nolan MA, Goldstein M, Basson CT, McKnight GS. Haploinsufficiency at the protein kinase A RI alpha gene locus leads to fertility defects in male mice and men. Mol Endocrinol 2006; 20:2504–2513.
62. Kamal A, Mansour R, Fahmy I, Serour G, Rhodes C, Aboulghar M. Easily decapitated spermatozoa defect: a possible cause of unexplained infertility. Hum Reprod 1999; 14:2791–2795.
63. Chenoweth PJ. Genetic sperm defects. Theriogenology 2005; 64:457–468.
64. Toyama Y, Iwamoto T, Yajima M, Baba K, Yuasa S. Decapitated and decaudated spermatozoa in man, and pathogenesis based on the ultrastructure. Int J Androl 2000; 23:109–115.
65. Baccetti B, Burrini AG, Collodel G, Magnano AR, Piomboni P, Renieri T, Sensini C. Morphogenesis of the decapitated and decaudated sperm defect in two brothers. Gamete Res 1989; 23:181–188.
66. Perotti ME, Giarola A, Gioria M. Ultrastructural study of the decapitated sperm defect in an infertile man. J Reprod Fertil 1981; 63:543–549.
67. Blom E, Birch-Andersen A. Ultrastructure of the "decapitated sperm defect" in Guernsey bulls. J Reprod Fertil 1970; 23:67–72.
68. Bugge TH, Kombrinck KW, Flick MJ, Daugherty CC, Danton MJ, Degen JL. Loss of fibrinogen rescues mice from the pleiotropic effects of plasminogen deficiency. Cell 1996; 87:709–719.
69. Ploplis VA, Carmeliet P, Vazirzadeh S, Van Vlaenderen I, Moons L, Plow EF, Collen D. Effects of disruption of the plasminogen gene on thrombosis, growth, and health in mice. Circulation 1995; 92:2585–2593.
70. Carmeliet P, Schoonjans L, Kieckens L, Ream B, Degen J, Bronson R, De Vos R, van den Oord JJ, Collen D, Mulligan RC. Physiological consequences of loss of plasminogen activator gene function in mice. Nature 1994; 368:419–424.
71. Mbikay M, Tadros H, Ishida N, Lerner CP, de Lamirande E, Chen A, El Alfy M, Clermont Y, Seidah NG, Chretien M, Gagnon C, Simpson EM. Impaired fertility in mice deficient for the testicular germ-cell protease PC4. Proc Natl Acad Sci U S A 1997; 94:6842–6846.
72. Catizone A, Ricci G, Galdieri M. Functional role of hepatocyte growth factor receptor during sperm maturation. J Androl 2002; 23:911–918.
73. Planes C, Caughey GH. Regulation of the epithelial Na+ channel by peptidases. Curr Top Dev Biol 2007; 78:23–46.
74. Hughey RP, Carattino MD, Kleyman TR. Role of proteolysis in the activation of epithelial sodium channels. Curr Opin Nephrol Hypertens 2007; 16:444–450.
75. Hernandez-Gonzalez EO, Sosnik J, Edwards J, Acevedo JJ, Mendoza-Lujambio I, Lopez-Gonzalez I, Demarco I, Wertheimer E, Darszon A, Visconti PE. Sodium and epithelial sodium channels participate in the regulation of the capacitation-associated hyperpolarization in mouse sperm. J Biol Chem 2006; 281:5623–5633.
76. Asnicar MA, Koster A, Heiman ML, Tinsley F, Smith DP, Galbreath E, Fox N, Ma YL, Blum WF, Hsiung HM. Vasoactive intestinal polypeptide/pituitary adenylate cyclase-activating peptide receptor 2 deficiency in mice results in growth retardation and increased basal metabolic rate. Endocrinology 2002; 143:3994–4006.
77. Sinclair S. Male infertility: nutritional and environmental considerations. Altern Med Rev 2000; 5:28–38.